Preparation of Porous Poly(oxymethylene) Membrane with High Durability against Solvents by a Thermally Induced Phase-Separation Method

HIDETO MATSUYAMA,[1] MASAKI KAKEMIZU,[1] TAISUKE MAKI,[1] MASAAKI TEARAMOTO,[1] KENJI MISHIMA,[2] KIYOSHI MATSUYAMA[2]

[1] Department of Chemistry and Materials Technology, Kyoto Institute of Technology, Matsugasaki, Sakyo-ku, Kyoto 606-8585, Japan

[2] Department of Chemical Engineering, Fukuoka University, 8-19-1 Nanakuma, Jyonan-ku, Fukuoka 814-0180, Japan

Received 27 October 2000; accepted 4 January 2001

ABSTRACT: Porous poly(oxymethylene) membranes were prepared as new solvent-resistant membranes by a thermally induced phase-separation method. Porous structures were formed by solid–liquid phase separation (polymer crystallization) rather than liquid–liquid phase separation. The pores existed in the intraspherulitic and interspherulitic regions. The effects of the polymer weight percentage and cooling rate on toluene permeance and solute rejection were investigated. The solvent resistance of the membranes was tested by the immersion of the membranes in organic solvents for 1 month, and high durability against the solvents was confirmed. © 2002 John Wiley & Sons, Inc. J Appl Polym Sci 83: 1993–1999, 2002

Key words: poly(oxymethylene) membranes; thermally induced phase separation; chemical resistance; polymer crystallization; membrane stability

INTRODUCTION

Microfiltration (MF) and ultrafiltration (UF) are important industrial processes, and the use of membrane separation processes has recently been increasing. However, polymer membrane materials are practical mainly for aqueous separations. Expanding the applications of MF and UF membranes leads to demands for their use in the field of organic separation. Furthermore, in membrane cleaning, specific cleaning solutions containing appropriate chemicals and/or detergents have been used.[1] The membranes are, therefore, required to have high durability against these chemicals.

UF membranes for nonaqueous use have been prepared from polyimide[2] and poly(*p*-phenylene terephthalamide).[3] Iwama and Kazuse[4] developed a solvent-resistant membrane for use in UF processes from newly synthesized polyimide. The membrane showed excellent stability and high fluxes with most common organic solvents, even when tested at elevated temperatures. In the three works just cited, the membranes were prepared by the immersion–precipitation method. That is, a homogeneous polymer solution was immersed in a nonsolvent bath. This means that these membranes inevitably had no durability against the solvents used in the preparation of the homogeneous polymer solutions. Recently, Fujii et al.[5,6] developed poly(phenylene sulfone)

Correspondence to: H. Matsuyama (matsuyama@chem.kit.ac.jp).

Journal of Applied Polymer Science, Vol. 83, 1993–1999 (2002)
© 2002 John Wiley & Sons, Inc.
DOI 10.1002/app.10147

(PPSO) hollow-fiber UF membranes. First, poly(phenylene sulfide sulfone) membrane was prepared by the immersion–precipitation method. The obtained asymmetric membrane was oxidized to PPSO membrane. The PPSO membrane had extremely high durability against solvents, heat, and oxidizing chemicals.

An alternative way to produce porous membranes is a thermally induced phase-separation (TIPS) process.[7–16] In this process, a polymer is dissolved in a diluent at an elevated temperature. Through cooling or quenching of the solution, phase separation occurs. Because the polymer is dissolved at a high temperature, TIPS is applicable to a wide range of polymers, including those that cannot be used in the precipitation method because of solubility problems. Porous membranes can be prepared by the TIPS process even from polymers that hardly dissolve in any solvents at room temperature and thus have high durability against the solvents. Mehta et al.[17] and Sonnenschein[18] reported the formation of microporous membranes via a TIPS process based on poly(ether ether ketone), which is a semicrystalline engineering thermoplastic with thermal and chemical resistance properties.

In this work, porous poly(oxymethylene) (POM) membranes were prepared by the TIPS process. POM is a crystalline engineering plastic with high chemical resistance. The solid–liquid phase separation (polymer crystallization) led to porous structure formation. The durability against many organic solvents was tested for the obtained membranes.

EXPERIMENTAL

Materials

POM was kindly supplied by Mitsubishi Engineering-Plastics Co. (Iupital® F10-01, copolymer type, melt index = 2.5 g/10 min). The diluent was diphenyl ether of a guaranteed reagent grade (Nacalai Tesque Co., Kyoto, Japan).

Phase Diagram and Spherulite Growth Rate

Homogeneous polymer–diluent samples were prepared by a method reported by Kim and Lloyd.[13] A 3–5-mg sample was sealed in an aluminum differential scanning calorimetry (DSC) pan, melted, usually at 453 K for 3 min, and then cooled at 10 K/min in a PerkinElmer DSC-7. The onset of the exothermic peak during cooling was taken as the dynamic crystallization temperature.

To check the existence of the cloud point, which is the border of liquid–liquid phase separation, we determined the temperature at which particle structures started to form with an optical microscope (Olympus, Tokyo, Japan; BX50). The polymer–diluent sample was placed between a pair of microscope coverslips. A Teflon film 200 μm thick with a circle opening in the center was inserted between the coverslips to prevent diluent loss by evaporation. The coverslip sample was heated on a hot stage (Linkam, LK-600PH) at 453 K for 1 min and then cooled at a controlled rate of 10 K/min with a Linkam L-600A controller. The temperature at which the particle structure formation occurred was recorded for various polymer concentration conditions.

The growth rate of sphere-shaped crystalline structures (spherulites) was measured by the hot stage. The experimental conditions were the same as those described previously, except for the cooling rate: three cooling rates of 1, 10, and 100 K/min were used. The image from the polarizing microscope was converted into a video signal that was passed through a video timer and into a video cassette recorder. To measure the spherulite size, we used image analysis. The image analysis software package was Win ROOF (Mitani Co., Fukui, Japan).

Membrane Preparation

Membranes used for the filtration experiments were prepared as follows. A homogeneous polymer–diluent sample was placed between a pair of glass plates (100 mm long, 100 mm wide, and 2.8 mm thick) or a pair of copper plates (150 mm long, 150 mm wide, and 0.5 mm thick). For adjusting the membrane thickness, we inserted a Teflon film 200 μm thick with a square opening in the center between the glass plates or copper plates. The plates were heated at 443 K in an oven for 30 min to cause melt blending. Then, the glass plates were cooled in air at room temperature, whereas the copper plates were quenched in ice water. Thus, the cooling rate for the copper plates was much higher than that for the glass plates. After cooling, the membrane was peeled from the plate and stored in toluene.

Scanning Electron Microscopy (SEM) Observations and Pore Size Measurements

In the membranes used for the filtration experiments and the membrane sample prepared with

the hot stage, the diluent was extracted with methanol, and the methanol was evaporated to produce the microporous membranes. The microporous membranes were fractured in liquid nitrogen and mounted vertically on sample holders. The surfaces of the samples were sputtered with Au/Pd *in vacuo*. A scanning electron microscope (Hitachi Co., Tokyo, Japan; S-2300) with an accelerating voltage of 15 kV was used to examine the membrane cross sections.

The pore size distributions of the membranes were measured with mercury porosimetry (Micromeritics Instrument Co., AutoPore III).

Filtration Experiments

The filtration experiments were performed with stirred cells made of Teflon that were similar to commercial stirred cells (Advantec Co., Tokyo, Japan; UHP-25K). First, the toluene permeance was measured. Then, to measure the solute rejection property with an aqueous solute solution, we immersed the hydrophobic POM membranes in toluene with 1 wt % sorbitan monooleate (surfactant), and subsequently, we passed propanol through the membranes before the filtration experiments. The permeance was almost the same before and after immersion in the surfactant solution. The feed aqueous solution was pressurized by nitrogen gas in the range of 2.0–3.0 atm. The solutes used were lysozyme from egg white (Seikagaku Co., Tokyo, Japan; 6X crystallized, molecular weight = 14,600, Stokes radius = 1.69 nm[19]), ovalbumin (Sigma Chemical Co., St. Louis, MO; grade V, 98% purity, molecular weight = 45,000, Stokes radius = 2.53 nm[19]), ferritin from horse spleen (Nacalai Tesque, Kyoto, Japan; molecular weight = 440,000, Stokes radius = 6.77 nm[19]), and polystyrene latex particle (Duke Scientific Co., Palo Alto, CA; radius = 50 nm). The feed solutions were prepared by the dissolution of the proteins in a 0.05 mol/dm^3 phosphate-buffered solution (disodium hydrogen phosphate and potassium dihydrogen phosphate, pH 7.0). The protein concentrations were 0.1 g/dm^3 for lysozyme, 0.2 g/dm^3 for ovalbumin, and 0.002 g/dm^3 for ferritin. The latex particle was dispersed in an aqueous nonionic surfactant (0.01% Triton X-100) at a concentration of 1.03×10^{11} particles/dm^3. The solute concentrations in the filtrate were measured with a UV spectrophotometer (Hitachi, Tokyo, Japan; U-2000) at wavelengths of 280 nm for lysozyme and ovalbumin, 275 nm for ferritin, and 385 nm for the latex particle.

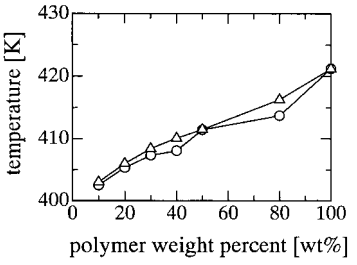

Figure 1 Phase diagram in the POM/diphenyl ether system: (○) the dynamic crystallization temperature and (△) the temperature at which particles were detected by optical microscopy.

To check the durability against solvents, we immersed the membranes in toluene, acetone, *N*-methylpyrrolidone (NMP), dimethyl sulfoxide (DMSO), ethanol, heptane, and ethyl acetate for 1 month. The toluene permeance and solute rejection coefficient for the latex particle were measured.

RESULTS AND DISCUSSION

Figure 1 shows a phase diagram for the POM/diphenyl ether system. The dynamic crystallization temperatures measured by DSC and the temperatures at which particles were detected by the optical microscope are plotted in this figure. The temperatures are almost identical, which indicates that particles were formed by the crystallization of POM. Therefore, an apparent binodal line, which is the border of the liquid–liquid phase separation, probably exists in the lower temperature region. Thus, the porous membrane structure was formed by solid–liquid phase separation (polymer crystallization) rather than by liquid–liquid phase separation.

Figure 2 shows images from the polarizing microscope during cooling. The spherulites grew as time passed. Finally, the spherulites impinged on one another, and all space was filled with the spherulites, although such an image is not shown in Figure 2.

The spherulite growth rates are shown in Figure 3 with changes in the polymer weight percentage in the solution and the cooling rate. The growth rate increased with decreasing polymer concentration. This was due to the high polymer mobility brought about by the decrease in the solution viscosity. Wang et al.[20] reported the opposite tendency, that is, a decrease in the growth

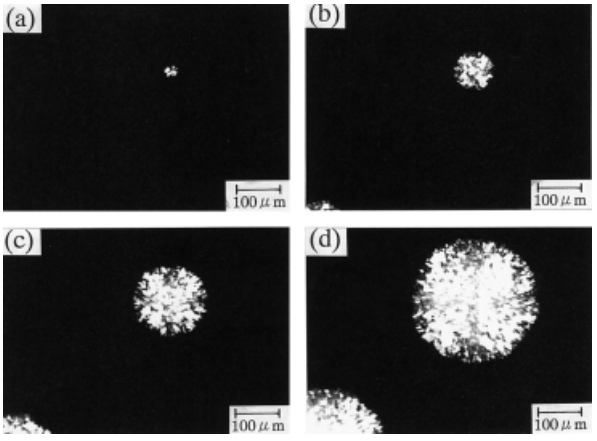

Figure 2 Polarized light micrographs of POM with a polymer concentration of 20 wt % and a cooling rate of 10 K/min: (a) 9, (b) 21, (c) 29, and (d) 37 s.

rate with the decrease in the polymer concentration in a binary mixture of POM and Novolak resin. The reason for this may be that the viscosity does not decrease so much with the addition of Novolak resin because the resin has a much larger molecule in comparison with that of the diluent used in this work. Figure 3(b) indicates that the spherulite growth rate was larger as the cooling rate became higher. The higher cooling rate led to more supercooling, which is defined as the difference between the equilibrium melting temperature and the actual crystallization temperature. The spherulite growth rate increased under the high supercooling condition.[21]

Figure 4 shows one example of a SEM photomicrograph of the cross section of the POM membrane. As can be seen in the enlarged micrograph, pores are formed in the intraspherulitic and in-

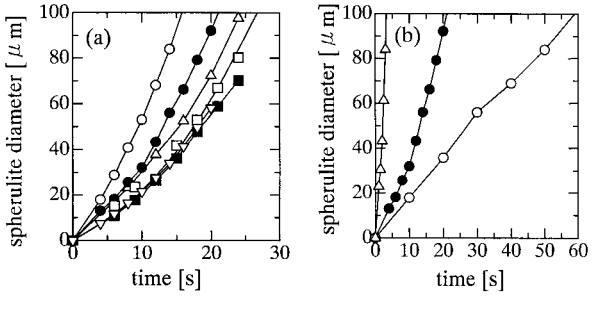

Figure 3 Time course of the spherulite diameter: (a) effect of the polymer concentration [(○) 10, (●) 20, (△) 30, (□) 50, (■) 80, and (▽) 100 wt %] with a cooling rate of 10 K/min and (b) effect of the cooling rate [(△) 100, (●) 10, and (○) 1 K/min] with a polymer concentration of 20 wt %.

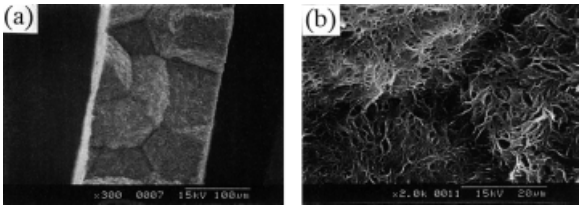

Figure 4 SEM photomicrographs of membrane cross sections with a polymer concentration of 40 wt % and a cooling rate of 10 K/min: (a) whole cross section and (b) enlarged photomicrograph.

terspherulitic regions. The pores in the intraspherulitic region are attributable to diluent entrapped within the spherulite structure. During spherulitic growth, the diluent is rejected to the interspherulitic region. This brings about the pores between the spherulites.

The pores in the intraspherulitic region are shown in Figure 5 for cases in which the polymer weight percentage and the cooling rate were changed. The pore size decreased with increasing polymer concentration because of the decrease in the volume fraction of diluent. A decrease in the cooling rate led to an increase in the pore size. As shown in Figure 3(b), the spherulite growth rate

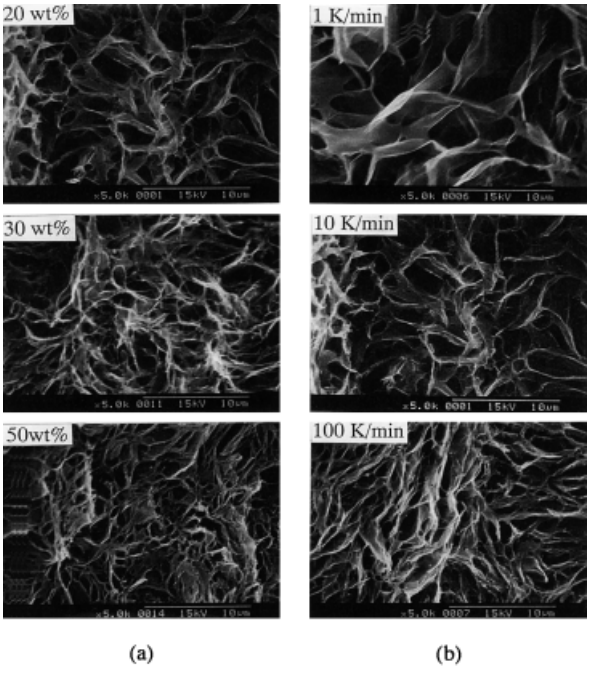

Figure 5 Membrane structure in the intraspherulitic region: (a) effect of the polymer concentration with a cooling rate of 10 K/min and (b) effect of the cooling rate with a polymer concentration of 20 wt %.

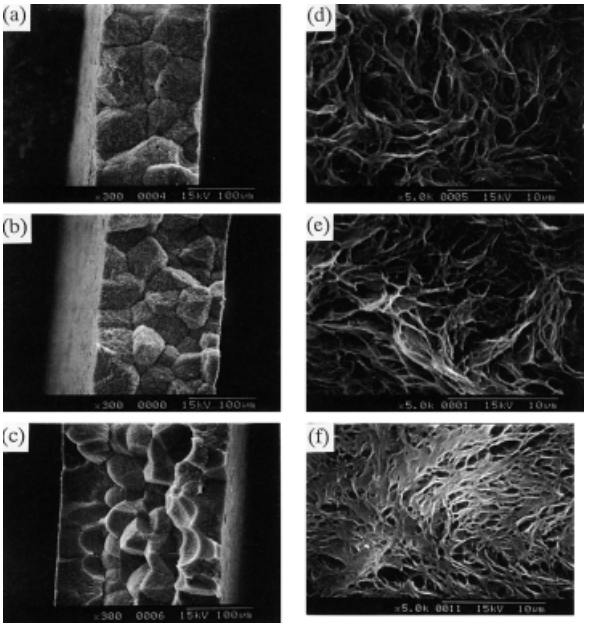

Figure 6 SEM microphotographs of the cross sections and intraspherulitic regions of the membranes used for the filtration experiments: (a–c): whole cross section and (d–f) intraspherulitic regions [(a,d) 30 wt % polymer concentration, cooled in air at room temperature; (b,e) 40 wt % polymer concentration, cooled in air at room temperature; and (c,f) 30 wt % polymer concentration, quenched in ice water].

was low with the low cooling rate. Thus, the diluent more readily concentrated during spherulite formation, and larger diluent domains were probably formed.

SEM microphotographs of whole cross sections and the intraspherulitic regions of the membranes used for the filtration experiments are shown in Figure 6. The spherulite size decreased with increasing polymer weight percentage because of increased spherulite impingement, which resulted from the increased number of nuclei formed.[13] The higher cooling condition led to an increased degree of supercooling, which also brought about the decrease in spherulite size due to the increased number of nuclei.[14] Although the difference between the 30 and 40 wt % samples is not so clear, with the increase in the polymer weight percentage and cooling rate, the pore size inside the spherulite decreased, which is in agreement with the results shown in Figure 5.

Figure 7 shows the pore size distribution measured with mercury porosimetry. The membrane used for the measurement was the same as that shown in Figure 6(c). The pore size ranged from

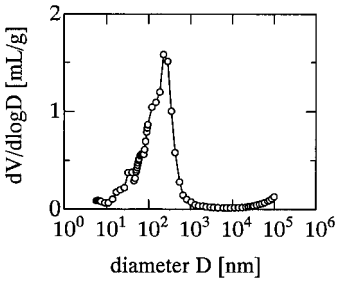

Figure 7 Pore size distribution for a membrane prepared with a polymer concentration of 30 wt % and quenched in ice water.

0.01 to 0.8 μm, and the average pore diameter was about 0.2 μm.

Figure 8 shows the relation between the toluene permeance and the polymer weight percentage. The toluene permeance is defined as the volumetric flow rate divided by the membrane area and the pressure difference. The ordinate is the permeance multiplied by the membrane thickness to correct the difference in the membrane thickness. The toluene permeance decreased with increasing polymer concentration. At the same polymer concentration, the permeance decreased with the higher cooling rate. As shown in Figure 4(b), pores existed in both the intraspherulitic and interspherulitic regions. The pores in the interspherulitic region seem to be somewhat larger than those in the intraspherulitic region. However, because the volume fraction of the interspherulitic region is much lower, the

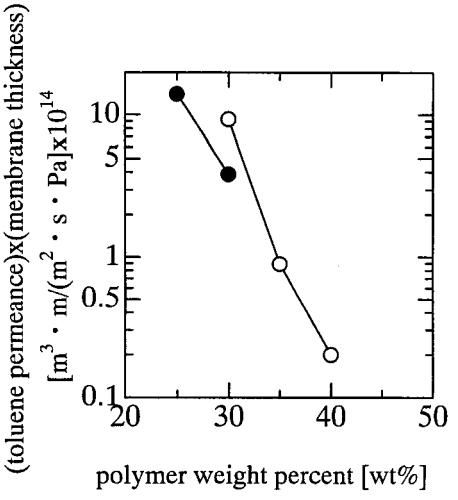

Figure 8 Relation between the toluene permeance and the polymer weight percentage: (○) cooled in air at room temperature and (●) quenched in ice water.

permeation property is mainly dominated by the pores in the intraspherulitic region. The pore sizes in this region decreased with the polymer concentration and cooling rate increasing, as shown in Figure 6. This is the reason that lower permeances were obtained with a higher polymer concentration and a higher cooling rate.

Figure 9 shows relations between the apparent solute rejection coefficient and the solute Stokes radius. The apparent solute rejection coefficient is defined as $1 - (C_f/C_0)$, where C_0 and C_f are solute concentrations in the feed and filtrate, respectively. The rejection coefficient increased with increases in both the polymer concentration [Fig. 9(a)] and the cooling rate [Fig. 9(b)]. This increase in the rejection coefficient was due to the decrease in the pore size shown in Figure 6. In a comparison of the results in Figure 9(a,b), the membrane prepared by quenching in ice water from a 30 wt % polymer solution showed rejection properties similar to those of the membrane prepared by cooling in air at room temperature from a 40 wt % polymer solution. However, the former membrane had better permeation properties because the toluene permeance for the former membrane was about 20 times higher than that for the latter membrane, as shown in Figure 8.

The toluene permeance and the solute rejection coefficient for the latex particle after immersion in the solvents for 1 month are summarized in Table I. The data are relative values for which the values before immersion were set to 100. The toluene permeance and the rejection coefficient were hardly changed by immersion in those organic solvents. Thus, high durability against the organic solvents was confirmed for the porous POM membranes prepared in this work.

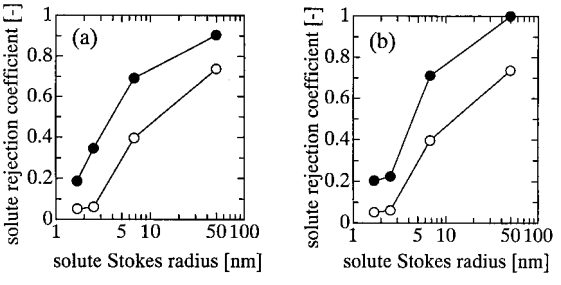

Figure 9 Relation between the apparent solute rejection coefficient and the solute Stokes radius: (a) effect of the polymer concentration [(○) 30 and (●) 40 wt %] with cooling in air at room temperature and (b) effect of the cooling condition [(○) cooled in air at room temperature and (●) quenched in ice water] with a polymer concentration of 30 wt %.

Table I Toluene Permeance and Solute Rejection Coefficient After Immersion in Solvents

Organic Solvent	Toluene Permeance (Relative Value)	Solute Rejection Coefficient for Latex Particle (Relative Value)
Toluene	98.3	99.1
Acetone	103	99.8
NMP	100	98.6
DMSO	96.0	99.7
Ethanol	101	101
Heptane	103	98.2
Ethyl acetate	97.8	99.1

Membrane preparation condition: polymer concentration = 30 wt %; cooling condition = quenched in ice water.

CONCLUSION

Porous POM membranes were prepared by the TIPS process. During cooling in the TIPS process, polymer crystallization occurred, and the spherulites that formed impinged on one another. Pores existed in the intraspherulitic and interspherulitic regions and were attributable to diluent entrapped within the spherulite and to diluent rejected to the interspherulitic region. The pores in the intraspherulitic region decreased with increases in both the polymer concentration and the cooling rate.

A higher rejection coefficient and a lower toluene permeance were obtained with the polymer concentration and cooling rate increasing. By immersing the membranes in organic solvents for 1 month, we tested membrane stability. The POM membranes had high durability against organic solvents.

The authors thank Mitsubishi Engineering-Plastics Co. for supplying Iupital® poly(oxymethylene).

REFERENCES

1. Zeman, L. J.; Zydney, A. L. Microfiltration and Ultrafiltration; Marcel Dekker: New York, 1996.
2. Strathmann, H. Desalination 1978, 26, 85.
3. Zschocke, P.; Strathmann, H. Desalination 1980, 34, 69.
4. Iwama, A.; Kazuse, Y. J Membr Sci 1982, 11, 297.
5. Fujii, Y.; Yamamura, H.; Noyori, M.; Nishimura, K. Membrane 1996, 21, 341.

6. Fujii, Y.; Yamamura, H.; Noyori, M.; Nishimura, K. Membrane 1996, 22, 285.
7. Castro, A. J. U.S. Pat. 4,247,498 (1981).
8. Caneba, G. T.; Soong, D. S. Macromolecules 1985, 18, 2538.
9. Hiatt, W. C.; Vitzthum, G. H.; Wagener, K. B.; Gerlach, K.; Josefiak, C. In Microporous Membranes via Upper Critical Temperature Phase Separation; Lloyd, D. R., Ed.; ACS Symposium Series 269; American Chemical Society: Washington, DC, 1985; p 229.
10. Lloyd, D. R.; Kinzer, K. E.; Tseng, H. S. J Membr Sci 1990, 52, 239.
11. Tsai, F.-J.; Torkelson, J. M. Macromolecules 1990, 23, 775.
12. Lloyd, D. R.; Kim, S.-S.; Kinzer, K. E. J Membr Sci 1991, 64, 1.
13. Kim, S.-S.; Lloyd, D. R. J Membr Sci 1991, 64, 13.
14. Lim, G. B. A.; Kim, S.-S.; Ye, Q.; Wang, Y.-F.; Lloyd, D. R. J Membr Sci 1991, 64, 31.
15. Vadalia, H. C.; Lee, H. K.; Myerson, A. S.; Levon, K. J Membr Sci 1994, 89, 37.
16. Matsuyama, H.; Berghmans, S.; Lloyd, D. R. Polymer 1999, 40, 2289.
17. Mehta, R. H.; Madsen, D. A.; Kalika, D. S. J Membr Sci 1995, 107, 93.
18. Sonnenschein, M. F. J Appl Polym Sci 1999, 74, 1146.
19. Matsuyama, H.; Iwatani, T.; Kitamura, Y.; Teramoto, M.; Sugo, N. J Appl Polym Sci 2000, 79, 2456.
20. Wang, X.; Saito, H.; Inoue, T. Kobunshi Ronbunshu 1991, 48, 771.
21. Ioue, K.; Okamoto, K.; Oguni, N.; Ochiai, H.; Satou, T.; Yasuda, H.; Yamashita, Y. Polymer Chemistry (in Japanese); Asakura Syoten: Tokyo, 1994.